

Chapter 3

Plasma-Catalyst Interactions



Hyun-Ha Kim, Yoshiyuki Teramoto, and Atsushi Ogata

Low-temperature catalytic reactions induced by nonthermal plasma (NTP) have been of great interest in plasma chemistry. The presence of plasma can alter the elementary steps in catalysis. The type of catalysts also provides substantial changes in plasma properties. This chapter reviews the current progress in the experimental observations and the understanding of bilateral interactions of NTP with catalysts. Among the various types of combinations, this chapter will mostly focus on the single-stage plasma-driven catalysis (PDC). Several lines of experimental evidence on the interaction are introduced: type of reactor, propagation of discharge streamer, key components of plasma, and catalyst durability.

3.1 From Plasma Alone to Plasma Catalysis

3.1.1 *Electrical Discharges and Plasma*

Electrical discharges can form plasma over a wide range of conditions: pressure, gas mixture, and temperature. In addition to various electrical discharges, electron-beam irradiation and gamma or X-ray also have a long history of being used over the past centuries. The latter is also referred to as radiation chemistry. Ozone generation by dielectric barrier discharge (DBD) has been a landmark of plasma applications in industry. From the 1980s, atmospheric pressure non-equilibrium plasma has gathered attention compared to the low-pressure (vacuum) plasmas. Pulsed corona discharges and DBD have been the two representative tools for generating NTP under mild conditions (i.e., ambient temperature and atmospheric pressure). Both

H.-H. Kim (✉) · Y. Teramoto · A. Ogata
National Institute of Advanced Industrial Science and Technology (AIST),
Tsukuba, Ibaraki, Japan
e-mail: hyun-ha.kim@aist.go.jp

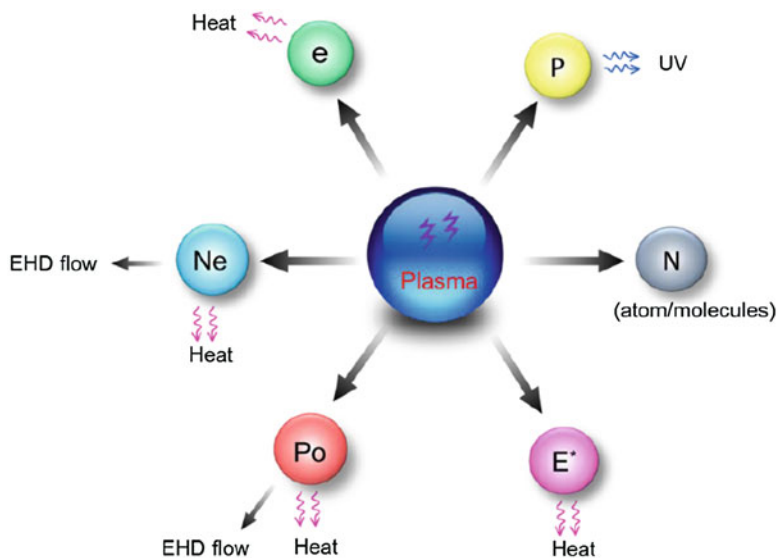


Fig. 3.1 Basic six particles in plasma: e electron, P photon, N neutrals (reactive species), E* excited molecules, Po positive ions, Ne negative ions [1]

electrical discharges and ionizing irradiation can generate plasma, which consists of six major particles, as shown in Fig. 3.1. Electron temperature (T_e) is often used to classify plasmas into “thermal” and “nonthermal.” In NTP, T_e is considerably higher than that of the ions (T_i) and ambient gas (T_g): $T_e \gg T_i \approx T_g$. These intrinsic advantages of NTPs attracted researchers to look at environmental remediation [2, 3], such as removal of NO_x and SO_x from flue gases [4–6], odor removal, and destruction of volatile organic compounds (VOCs) [7] or hazardous air pollutants (HAPs). Extensive studies in the 1990s shed light on the merits and demerits of using NTP processes for environmental applications [4, 7, 8]. The demerits include high energy consumption and the formation of unwanted byproducts [9, 10]. Plasma catalysis has been proposed as one of possible alternatives to pure plasma processes. The interaction of these six particles and the catalyst will be discussed in Sect. 3.3.

Early reports on the catalytic effect of electrode materials in corona discharges may date back to the 1920s [11]. Figure 3.2 illustrates the scheme on how O_3 formation is suppressed by the catalytic action of electrode materials. Silver was found to be most prominent in O_3 suppression. Later, these effects were found to be related with the electrode oxidation/reduction of electrode surface (aging condition) and catalytic activity toward O_3 decomposition [12–14]. For example, it has been reported that an O atom fixed on Ag (Ag-O) can catalytically convert O_3 to O_2 [15], which may explain the O_2 suppression with an Ag electrode. Sporadic studies have been reported over several decades [16], and studies on plasma catalysis became widespread after 2000. Surface-plasma interactions have also been found in plasma-enhanced chemical vapor deposition (PE-CVD), sputtering, and plasma etching, but

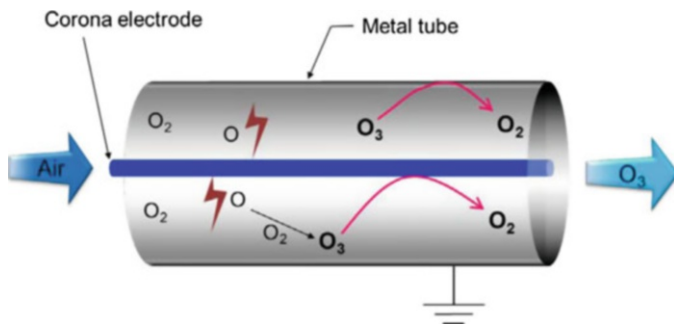


Fig. 3.2 Catalytic decomposition of O_3 on the surface of electrodes [12]

these processes are usually operated at low pressure or vacuum, whereas the pressure range of plasma catalysis is basically atmospheric pressure.

3.1.2 Beyond the Incompatibility

In principle, low temperature and high activity are completely incompatible in conventional catalysis. The most important issue in plasma catalysis is the low working temperature below or near the light-off temperature in catalyst-alone processes. This temperature isolation can make the two processes cooperative rather than having a competitive relationship. The combination of NTP and catalyst aims to achieve a synergistic effect, which enables better removal efficiency, selectivity, and carbon balance [17–20]. Plasma can generate highly reactive chemical species (both oxidative and reductive) even at ambient temperature and pressure. This complementary combination is the essence of a plasma-catalyst. Plasma enables catalysts to be effective at lower temperatures. Catalysts provide a better selectivity by providing new chemical pathways via surface reactions. There is a large body of literature reporting synergistic effects in plasma catalysis [1]. However, some of the results were obtained under extremely high specific input energy, where the heating is not negligible (see also Sect. 3.3.4). The number of catalysts (combinations between active metals and supports) tested for plasma catalysis is rapidly increasing, but there still exists tremendous number of catalysts hitherto unstudied. Even for a given combination, catalytic activity changes depending on the loading amount, size, and redox condition of active metals. A number of reviews and references are available for the applications of plasma catalysis, which include steam reforming [21], dry reforming with CO_2 [22, 23], CO/CO_2 methanation [24], hydrogenation of CO_2 [25], de- NO_x [26–31], NO_x synthesis [32], NH_3 synthesis [33–35], volatile organic compound (VOC) removal [36], and water purification [37]. This chapter will mostly discuss the lateral interactions between plasma and catalyst to draw the best guideline available as of now.

3.2 Plasma Catalysis Reactors

3.2.1 Reactor Classification

Classification of plasma catalysis reactors is usually based on the position and number of catalysts. Figure 3.3 schematically illustrates the typical reactors used in plasma-catalyst studies. The single-stage reactor (Fig. 3.3(i)), where catalysts are located inside the plasma zone, is also referred to as plasma-driven catalysis (PDC) or in-plasma catalysis (IPC). The term “PDC” was first used in 1999 to describe the combined process of pulsed corona and TiO₂ catalyst for the removal of NO_x [38]. The presence of a dielectric barrier (glass, ceramic, quartz, etc.) can prevent a transition into a spark discharge. Bilateral interactions between plasma and in PDC reactor impose difficulties in understanding the elementary processes. Each elementary property becomes interdependent when catalysts are placed in the plasma zone. In contrast, catalysts are located downstream of the plasma reactor in the two-stage reactor (Fig. 3.3(ii)). In chemical viewpoint, short-lived radicals (O(³P), O(¹D), OH, N) cannot be utilized in the two-stage configuration. Ozone-assisted catalysis is one of the most well-known two-stage reactors. A multi-stage process (Fig. 3.3(iii)) could be an interesting option for the industrial application. The most important aspect is that each catalyst has a different function along the flow direction, which can be fine-tuned for specific purposes [39–42]. Further oxidation of byproducts or intermediates and reduction of O₃ could be optimized by using multi-stage configurations.

The VOC oxidation in single-stage PDC was found to be accelerated by increasing O₂ content in the gas mixture [43, 44] while this trend is not observable in either pure plasma or catalyst processes. The cycled system for VOC oxidation (Fig. 3.3(iv)) is based on this unique O₂-dependent behavior. The operation of the cycled system is quite similar to the conventional adsorption, except for the catalyst regeneration using oxygen plasma. Once the catalyst bed reaches adsorption saturation, the catalyst bed is purged with pure O₂ and then plasma is turned on to decompose adsorbed VOCs. The primary advantages are the fast and energy-efficient reduction/oxidation under highly controlled environment (i.e., pure O₂ or N₂). Many recent studies confirmed the advantage of the cycled system for the removal of benzene [45–47], toluene [48–51], and HCHO [52] using a variety of adsorbent/catalyst combinations. Adsorption followed by treatment with air plasma can also enhance the energy efficiency of VOC removal [53–55]. However, NO_x formation is inevitable in air, so the input power (i.e., treating capacity) should be carefully considered to meet the regulation of NO_x emission. Oxygen plasma instead completely suppresses NO_x formation during the oxidation of adsorbed VOCs. TiO₂ is a highly sensitive catalyst to O₂ content, but the low adsorption capacity limited its potential for the cycled system. Despite the large surface area and the well-established performance, activated carbon is not suitable for the cycled system due to its electrical conducting nature (electrical resistivity of ~10⁻¹ Ω-cm) [56]. Up to

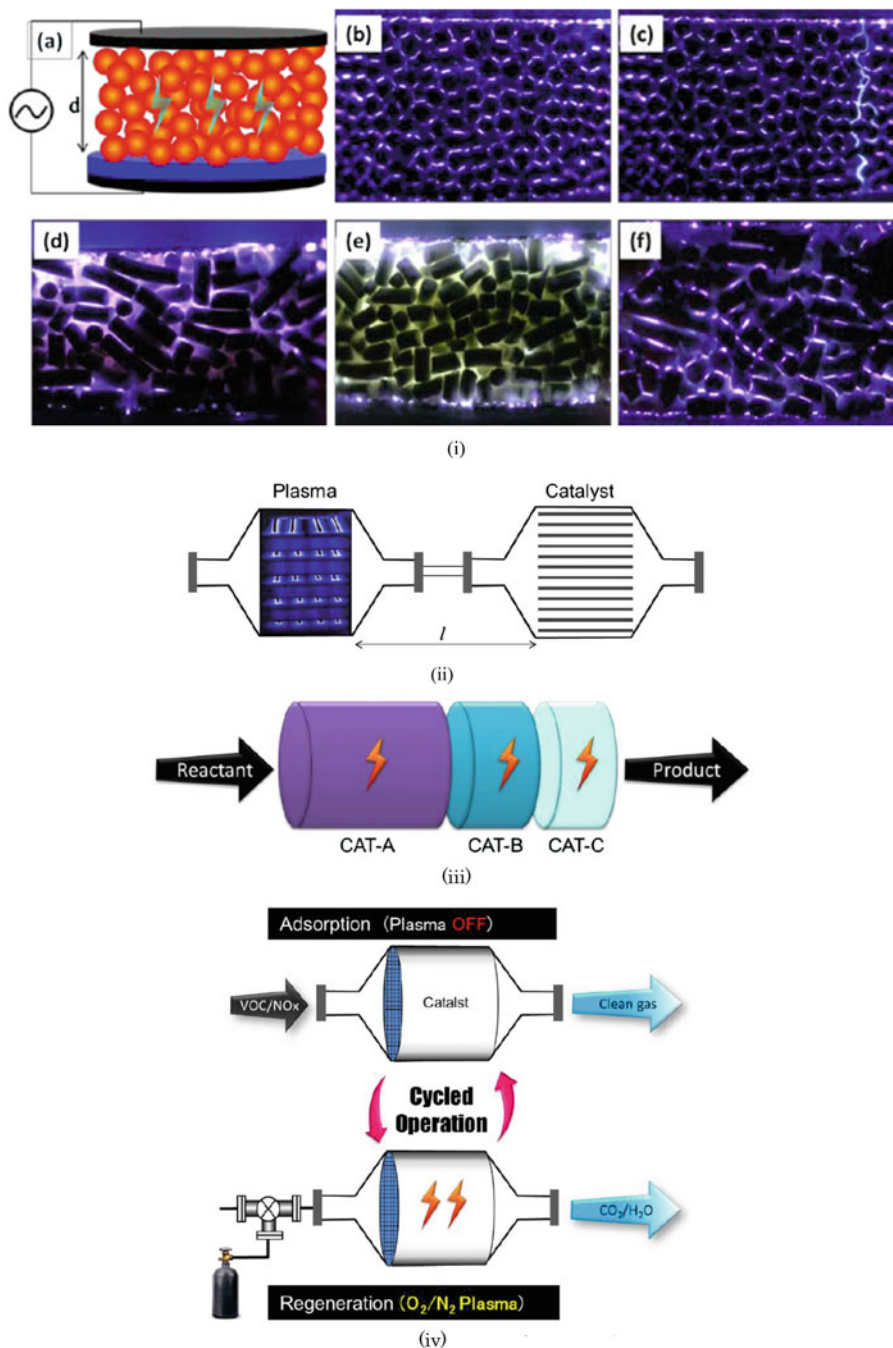


Fig. 3.3 Plasma-catalyst reactors. (i) Single-stage plasma-catalyst reactor. (a) Typical plane-type packed bed reactor, (b) BaTiO₃ (plasma on), (c) BaTiO₃ (plasma with spark discharges), (d) bare HY, (e) 2 wt% Ag/HY, (f) 5 wt% Ag/Ms-13X (b~f, mesh-to-mesh electrode) (ii) Two-stage plasma-catalyst reactor. (iii) Multi-stage plasma-catalyst reactor [1]. (iv) Cycled system (adsorption ↔ regeneration using O₂ or N₂ plasma)

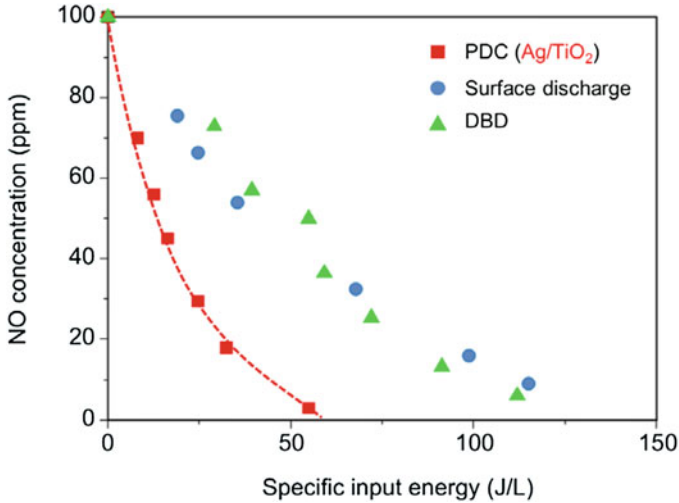


Fig. 3.4 Comparison of PDC and plasma alone (surface discharge, DBD) in NO removal in N₂ at 373 K. Energy constant k_E for the PDC and plasma-alone reactors were $49 \pm 1 \times 10^{-3}$ L/J and $19 \pm 4 \times 10^{-3}$ L/J, respectively [60]

date, metal nanoparticle-loaded zeolites satisfy the requirements of the cycled system: adsorption capacity and high catalytic activity under an O₂ environment.

A cycled system has been studied for NO_x reduction into N₂ [57–59]. In these cases, N₂ plasma is used to form N atoms for NO_x reduction. It is interesting to see that PDC is also superior to plasma-alone process as shown in Fig. 3.4 for the removal of 100 ppm of NO in N₂. Comparison of the energy constant k_E revealed [60] that the PDC reactor packed with Ag/TiO₂ catalyst showed 2.6 times more efficiency than the pure plasma reactor. Fixation of radicals on the surface of catalyst and its chemical reaction are further discussed in Sect. 3.3.3.

3.2.2 Equivalent Electrical Circuit

The physicochemical parameters of catalysts (i.e., loading material and their size distribution, supporter, pore size, void volume, surface area, etc.) are important parameters in determining the catalytic activity. Except for activated carbon, most of catalytic materials are electrically insulating. In contrast to a two-stage reactor, resistivity, capacitance, and dielectric constant of catalysts are key components in a single-stage plasma-catalyst reactor. Figure 3.5 illustrates the electrical equivalent circuit of (a) dielectric-barrier discharge and (b) single-stage plasma-catalyst reactor. In general, DBD is represented by the bipolar Zener diode [62] or time-varying resistance $R(t)$ [63]. In the case of a single-stage plasma-catalyst reactor, the resistance (R_C) and capacitance (C_C) of the catalyst are connected in series to the air gap.

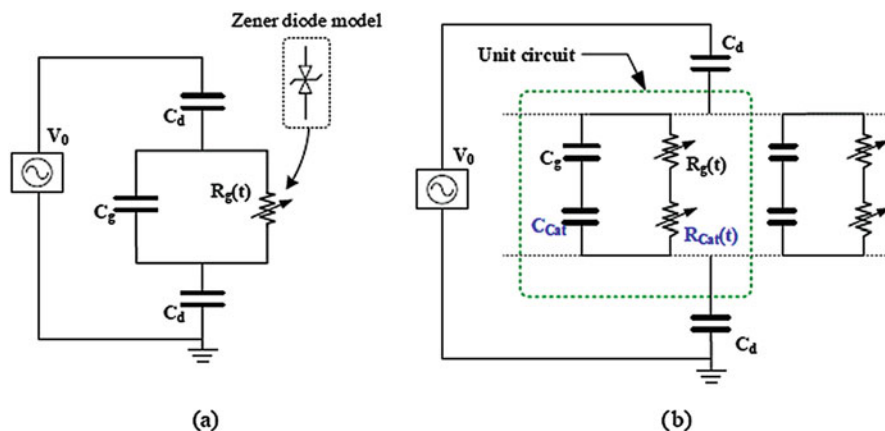


Fig. 3.5 Equivalent electrical circuit of plasma-catalyst reactor [61] (a) DBD reactor, (b) Single-stage plasma-catalyst reactor

This capacitance in series divides the applied voltage on the air gap more, which leads to a favorable condition for partial discharges at the contact points of catalysts. Plasma onset voltage is usually lowered when catalysts are packed in DBD reactors [64]. This can be simply explained by the reduced gap distance between the contact point of catalyst pellets. Dielectric constant of packing materials also influences the discharge power and plasma onset voltage [65]. In other words, changing packing material from one to another can alter the equivalent circuit and the plasma generation. A Lissajous figure and current waveforms are handy methods to monitor the change in the plasma properties [66]. When Ag was impregnated on a given framework of HY zeolites, the oxidation state of Ag substantially changed according to the Si/Al ratio. The higher the Si/Al ratio, the larger the drop of electrical resistivity, in turn leading to a diminished propagation of surface streamers [67]. This observation clearly indicated that the electrical parameters of each of the packing materials are highly important in determining not only the propagation of surface streamers but also the catalytic activity under oxygen plasma.

3.2.3 Use of Plasma for Catalyst (Preparation, Reaction, and Regeneration)

Plasma can be utilized for catalysis in three different ways: preparation, reaction, and regeneration. Firstly, plasma is used for catalyst preparation such as precursor decomposition [68], template removal [69], reduction of active metal nanoparticles [70, 71], and stable dispersion [72]. A group from Tianjin University studied the effects of glow plasma in the preparation of various catalysts and reported enhanced dispersity and higher activity [68, 73]. Menard et al. compared thermal and ozone

treatments for the removal of the protecting ligand in Au cluster catalysts [74]. They reported that the ozone-treated Au/TiO₂ showed smaller mean diameter, higher activity, and better thermal stability. Residual chloride in the prepared catalyst is a poison of active site, so subsequent treatment is a crucial step before use. Secondly, plasma can enhance catalytic reactions, which is the key aspect in single-stage PDC reactor. Details of the plasma effect on catalysis will be discussed in Sect. 3.3.

Thirdly, regeneration of the catalyst could be also achieved by NTP. Plasma regeneration strongly depends on the type of deactivation. When the coverage by organic substances is the main cause of deactivation, there is a possibility for plasma to be effective. Low-pressure glow discharge in Ar-O₂ mixture was found to be effective for the decoking of catalysts [75, 76]. Nano-sized Au catalysts are well-known for high activity toward CO and H₂ oxidation at room temperature, or even down to below 200 K. The high catalytic activity for CO oxidation quickly drops when Au/TiO₂ is exposed to 100 ppm of toluene or C₃H₆ [77]. Heating is not suitable for a nano-sized Au catalyst due to the thermal agglomeration of Au particles that eventually leads to irreversible deactivation. However, oxygen plasma can regenerate Au/TiO₂ catalyst at ambient temperature [77, 78]. Interestingly, plasma can promote CO oxidation over the fully deactivated Au/TiO₂ catalyst by the adsorption of hydrocarbons (propylene and toluene). Plasma can directly supply reactive oxygen species to the surface of Au from the gas phase leading to the oxidation of CO. We referred to this type of reaction as a “reverse Eley-Rideal”-type reaction [1]. In this case, plasma not only regenerates the deactivated surface but also promotes the chemical reaction.

The shape of supported metal catalysts is known to change according to reaction conditions. Recently, Yoshida et al. visualized the shape change of Au on CeO₂ by means of aberration-corrected ETEM (environmental transmission electron microscopy) [79]. Plasma can form strongly oxidative or reducing conditions depending on the gas mixture. This transient behavior will be an interesting subject worth studying in the future.

3.2.4 Elementary Steps in Plasma Catalysis

Both conventional and plasma catalysis consist of the common elementary steps: adsorption and surface diffusion of reactants, surface reaction, and desorption of products. The characteristic difference between them is the driving force, i.e., heat vs plasma. Each of these elementary steps influences the overall reaction rate. In many cases, catalytic reactions are kinetically expressed by the Langmuir-Hinshelwood (L-H) mechanism as shown in Eq. (3.1). The reaction rate coefficient k can be expressed by the Arrhenius Eq. (3.2)

$$r = -\frac{dC}{dt} = \frac{kKC}{1 + KC} \quad (3.1)$$

$$k = A \exp\left(-\frac{E_a}{RT}\right) \quad (3.2)$$

E_a and K denote the activation energy and equilibrium constant, respectively. The smaller the E_a and the higher the T , the larger the reaction rate coefficient k becomes. The presence of plasma can alter these four factors (k , K , E_a , and T), which eventually leads to synergistic effect in plasma catalysis. Clearly, plasma provides new elementary steps to catalysis, which in turn leads to either a larger k by decreasing E_a or a better selectivity. It should be noted that the Arrhenius equation is based on a state in thermal equilibrium while plasma catalysis is in a non-equilibrium state. In this sense, careful attention should be paid before implementing an Arrhenius plot to the data analysis for plasma catalysis.

3.3 Players in Catalyst Activation

3.3.1 Time-Scale Matching

Figure 3.6 compares the characteristic time scales of the elementary processes in plasma and catalytic reactions. Microdischarges in DBD and streamers in pulsed corona have a typical duration of 10^{-8} s, which can be easily monitored by current waveforms. Excitation and electron-impact dissociation lead to formation of reactive

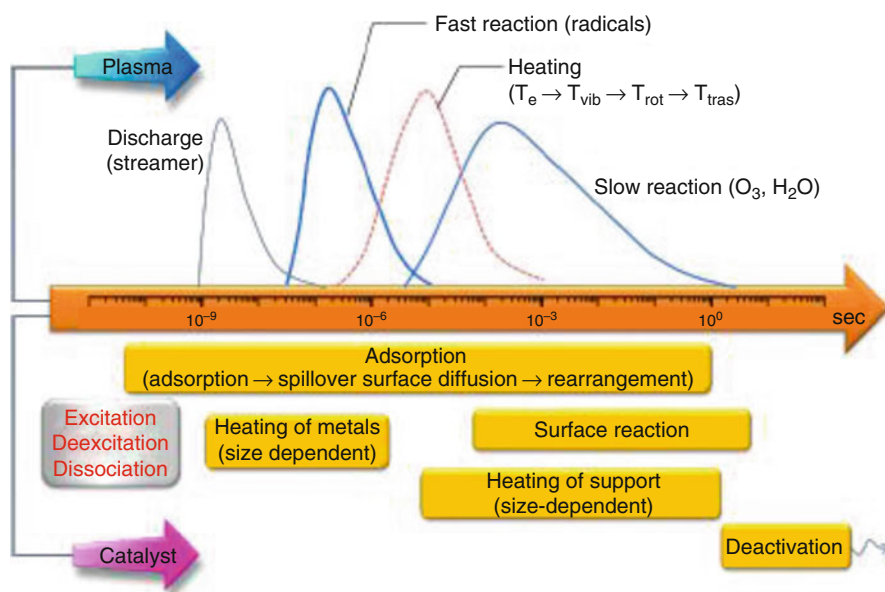


Fig. 3.6 Characteristic time scales in plasma and catalytic reaction [1]

species. Radical reactions have typical time scales of 10^{-5} s, and recombination of radicals yields relatively stable species (O_3 and H_2O_2) which contributes to slower reaction times. In a catalytic reaction, the initial chemisorption step occurs within 10^{-9} s. However, the total adsorption process proceeds over a significantly longer time scale (up to 100 s), as a result of surface rearrangement via spillover and surface diffusion, along with gas-phase diffusion into the micropores. The catalytic turnover time scale is known to be in the range of 10^{-2} to 10^2 s [80], which is slower than the fast radical reactions by a factor of 2–3 orders of magnitude. This different time scale suggests that the rate-limiting step is a surface reaction rather than a plasma-involved process in the gas phase.

3.3.2 *Less Important Particles (Electrons, Photons, and Ions)*

As illustrated in Fig. 3.1, plasma chemistry is the combined actions of the six major particles. Among them, neutral atoms (i.e., radicals) and molecules (O_3 , H_2O_2) are generally believed to play a key role in most of the chemical reactions. The electron density and its energy distribution have been studied intensively in order to understand the physical properties of plasmas. Ion chemistry (ion molecules) proceeds even faster than radical reactions, but their direct contributions to the overall reaction are considered to be negligible due to the dilute concentration of pollutants [21]. In a typical gas composition, i.e., air containing pollutants in ppm level, most of electron energy is preferentially transferred to the dominant gases (O_2 and N_2), which leads to the formation of reactive species.

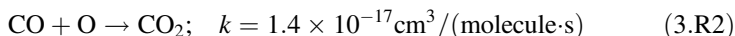
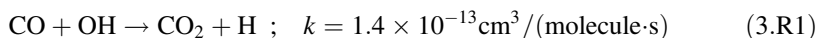
Various methods of optical diagnostics have been developed and noticeable advancements have been made during the last decade. Optical emission spectroscopy (OES) has indicated that plasma in an air-like mixture produces UV light, which has potential to activate catalysts. This qualitative information led researchers to speculate the contribution of UV light as a possible reason for synergistic effects in plasma catalysis [38]. The solar flux on the Earth's surface is about 100 mW/cm^2 (137 mW/cm^2 at the top of the atmosphere, solar constant), and the UV flux occupies about 7 mW/cm^2 . Recent quantitative measurements of UV photon flux in air revealed that it is only on the order of several $\mu\text{W/cm}^2$ [81–83], which is about three orders of magnitude less than that of the outdoor solar UV flux. The contribution of UV light in plasma catalysis is a matter of the UV photon flux, but not the mechanism itself. When external UV with a photon flux of several tens mW/cm^2 was used to irradiate a plasma-catalyst reactor, a measurable enhancement was observed [84, 85].

3.3.3 Important Particles (Radicals, Excited Molecules)

The formation and contribution of various radicals ($O(^3P)$, $O(^1D)$, OH , N) and reactive molecules (O_3 , H_2O_2) have been considered key factors in determining the plasma chemistry. Laser diagnostics have been implemented to measure time- and space-resolved formation and decay of these reactive species [86].

Radical fixation on the surface of a catalyst is a unique pathway in plasma catalysis. Generally, the lifetime of radicals in gas phase lies in the order of 10^{-5} s, but the surface-fixed species can survive over several tens of minutes [87–89] or even hours [90]. Guaitella et al. studied adsorption/reaction kinetics of C_2H_2 on the surface of plasma-treated SiO_2 and TiO_2 catalysts and found that O_2 or air plasma-pretreated TiO_2 can remove C_2H_2 while no removal occurred with the SiO_2 catalyst [87]. The NO measurement using in situ tunable diode laser absorption spectroscopy (TDLAS) revealed that RF plasma pretreatment can fix N atoms (in N_2) [88] or O atoms (in synthetic air) [91] on Pyrex which were stable over several tens of minutes.

Carbon monoxide (CO) is one of the major byproducts in VOC removal. CO oxidation in gas phase is limited due to the slow reaction rate coefficients.



Ozone has quite poor reactivity in gas phase with most of the chemicals, except for hydrocarbons containing a $C=C$ double bond. However, the long lifetime of ozone enables a two-stage configuration. Furthermore, ozone-metal interactions can modify its reactivity. For example, Au-O is formed when nanoporous Au is exposed to O_3 , even at room temperature. Biener et al. demonstrated that ozone-induced oxygen uptake is only limited to a monolayer rather than fully oxidizing the nanoporous Au [92]. The Au-O successfully oxidized CO into CO_2 .



Excited molecules exhibit a much larger reactivity when compared to the ground state. The contribution of vibrationally excited molecules has also been discussed in surface chemistry [93]. Nozaki et al. reported that vibrationally excited methane could be used to improve dissociative chemisorption on Ni/SiO_2 catalyst [21, 94].

3.3.4 Additional Effect (Heat)

In principle, plasma activates catalysts in plasma catalysis in the same way as heat, when looking at conventional catalysis. The electrical energy injected into plasma reactors is eventually converted into heat, so the temperature increase is a function of how much energy has been injected into a given reactor. Heat released from plasma can also play a role in plasma catalysis. The sources of heat in plasma catalysis can be divided into electrical and chemical factors. Electrical factors include both dielectric loss in barrier and catalysts and joule heating by the current flow. Chemical effects are a combination of vibrational-vibrational (V-V) and a vibrational-translational (V-T) relaxation, as well as the heat of reactions (i.e., exothermal reactions). The heat of a reaction is in the range of several thousand kJ/mole. However, the concentration of organic pollutants is usually in several hundred ppmv level, so its contribution to heating process is not significant in treating dilute VOCs. The degree of heating is primarily dependent on the power input into a plasma reactor. The measured rates of temperature increase were determined to be approximately 30~40 K per 100 J L⁻¹ [61]. The gas temperature and gas composition change along the flow direction, so the main reactions can be sectionalized from inlet to outlet. The inlet section should be effective for the initiation reaction, while the middle and end parts are for intermediates and unwanted byproducts (CO or O₃). In the case of VOC oxidation, the usual intermediates are aldehydes and CO. Some catalysts exhibit even higher activity toward these intermediates than the reactants. It is therefore expected that contribution of thermal catalytic reaction can vary with the position.



For example, decomposition of aromatic hydrocarbons requires temperatures of about 473 K. Specific input energy of 200 J/L in air leads to a temperature increase of about 75~95 K. This temperature is far less than that required for the thermal catalysis of most of aromatic compounds but sufficient for the light-off of CO oxidation (threshold temperature for CO oxidation). The Au catalyst on the oxide supports (TiO₂, CeO₂, and Fe₂O₃) is a well-known catalyst for CO oxidation, even at temperatures as low as 200 K [95]. Jiang et al. reported the complete oxidation of C₂H₄ over a Pt/MCM-41 catalyst at room temperature [96]. These results clearly suggest that the heating effect in plasma catalysis should be considered as depending not only on the substances under reaction but also on the type of catalysts. From the perspective of reactor design, a heat-tight configuration will be highly important for endothermic reactions, while cooling will be beneficial for exothermic reactions [1].

3.3.5 Probing Interaction of Plasma and Catalyst

Despite the various experimental approaches, a clear understanding of the mechanism is still elusive. The development of in situ measurement techniques has played an important role both in catalysis and NTP studies. However, the use of these well-established in situ techniques in catalyst study (such as in situ X-ray powder diffraction (XRD) with heating and gas flow, diffuse reflectance infrared Fourier transform spectroscopy (DRIFTS), and in situ Raman spectroscopy) is hampered in plasma catalysis due to the presence of high-voltage and electromagnetic noise. Recently, DRIFTS has been used in measuring plasma-induced surface reactions, such as hydrocarbon-assisted selective catalytic reduction of NO_x [97] and VOC decomposition over three metal oxides ($\gamma\text{-Al}_2\text{O}_3$, TiO_2 , and CeO_2) [98]. Plasma-induced fixation of oxygen species over Ag-supported TiO_2 and MS-13X was studied using isotopically labeled oxygen ($^{18}\text{O}_2$) and an online mass spectrometer [89]. The amount of surface-fixed oxygen species was proportional to the amount of Ag loaded, and their lifetimes were found to be up to 10 h, based on the NO titration method [90].

Laser-induced fluorescence (LIF) has been used in the nondestructive diagnostics of reactive species with a high sensitivity [86]. Su et al. used a planar LIF imaging and near-IR thermography for high-throughput screening of active catalysts for naphthalene oxidation by detecting fluorescence signals using a CCD camera [99, 100]. A total of 15 catalyst samples were mounted in a flow cell reactor heated at 503–643 K; the fluorescence emissions of 515–546 nm from the reaction product (naphthoquinone) were measured just above the catalysts. Application of these techniques in plasma catalysis may accelerate the progress of plasma catalysis by providing fast and high-throughput screening of catalysts.

3.4 Discharge Characteristics and Surface Streamers

3.4.1 Surface Streamers

Two characteristic discharge modes are found in a catalyst-packed plasma reactor: partial discharge (PD) and surface streamers [101, 102]. Partial discharge consists of numerous microdischarges at the contact points of catalysts where the electric field is augmented due to large dielectric constants of the packing materials [65, 103–105]. The PD appears as a spot, and its size becomes larger as the applied voltage increases. The second type of discharge is surface streamers. Propagation of surface streamers was found to highly correlate with performance of plasma catalysis [101]. This kind of correlation is a new insight hitherto never considered. Investigation of a surface streamer requires an intensified CCD camera because of its low intensity. Figure 3.7 compares three random images of plasmas in air in the absence (a) and the presence of Ag nanoparticles (b and c). In the case of bare MS-13X (a),

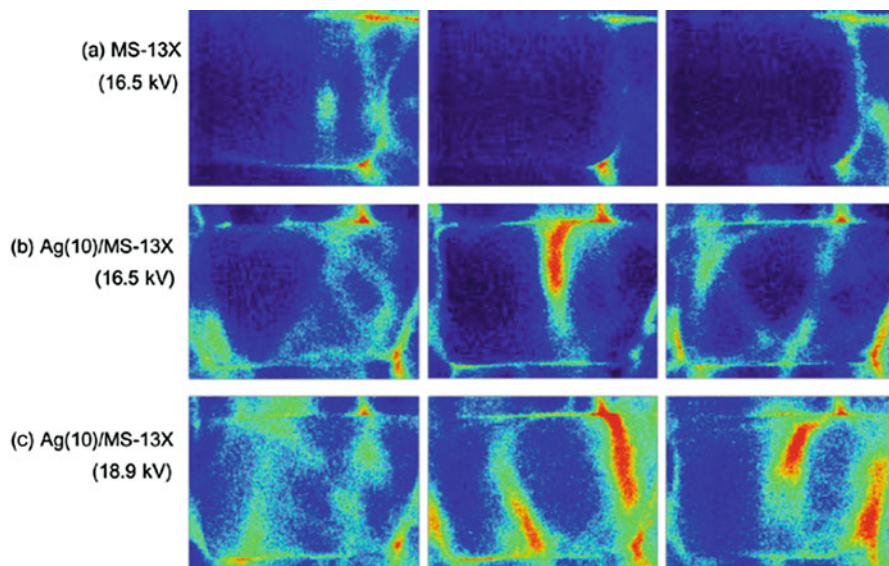


Fig. 3.7 Three random images of plasma generation for (a) bare MS-13X (16.5 kV) and (b and c) Ag(10)/MS-13X. Frequency and ICCD gate time were 50 Hz and 10 ms, respectively

PD was dominant at contact point of pellets, and surface streamers appeared in limited number and position. On the other hand, surface streamers became dominant for the Ag(10)/MS-13X (b and c). Of course, the bare MS-13X exhibits poor VOC removal, CO₂ selectivity, and carbon balance. A considerable enhancement can be made when Ag nanoparticles are loaded on the MS-13X. This physical interaction is a completely new category determining the catalytic activity.

Figure 3.8 shows the ns-gated images of surface streamers propagating on the bare γ -alumina. Total emission (b) and N₂(C) emission (c) obtained with a band-pass filter showed a similar pattern. N₂(C) emission, which is also referred to as second positive band of N₂(C³ Π_u) \rightarrow N₂(B³ Π_g) transition, requires threshold energy of 11 eV. In an air-like discharge, the N₂(C) emission at 337.1 nm is the most prominent line regardless of the type of plasma reactor. A distinctive feature of the surface streamers was a sheet-like flat structure with a width of about 500 μ m, which is different from the gas-phase streamer. Gas-phase streamer appearing at the gap of neighboring pellets in (b) had a diameter of about 150 μ m, which is consistent with literature values for barrier discharge [106, 107].

Figure 3.9 shows a sequence of surface streamers on a 2 wt% Ag/TiO₂ catalyst up to 14 ns. The primary streamer (PS) started not only from the tip of the point electrode but also from the catalyst contact points along the needle electrode. When the PS reached a contact point with the next bead, the discharge intensity became stronger by merging the PS1 and PD at 6 ns. These observations clearly indicated that PD can be a staging point during the propagation of surface streamers over multiple catalyst beads. Propagation velocity of PS was about 250 km/s at 7.1 kV and increased linearly with the applied voltage. However, it is much slower than those reported values for PS (500–3000 km/s) in gas phase [107, 109–111].

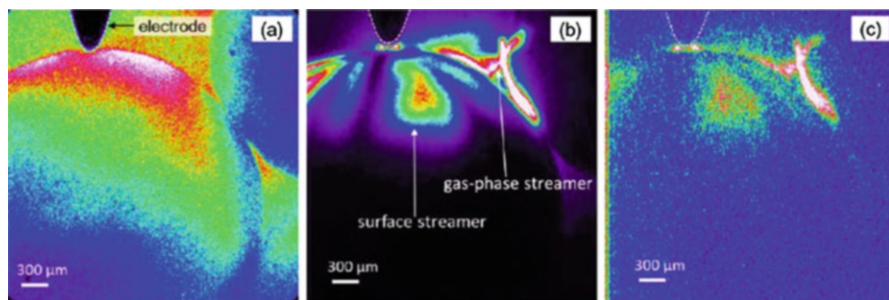


Fig. 3.8 Surface streamers on bare alumina with a point-to-plate configuration: (a) observation area (without discharge), (b) total emission, and (c) excited N_2 emission of $N_2(C_3\Pi_u) \rightarrow N_2(B_3\Pi_g)$ transition at 337.1 nm (the second positive band). Applied voltage was 9.3 kV

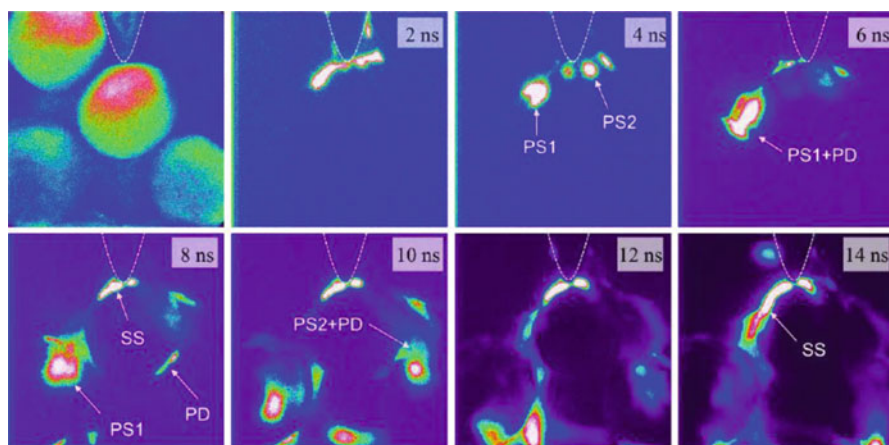


Fig. 3.9 Time-resolved images of surface streamer on $Ag(2)/TiO_2$ catalyst (at 7.1 kV, 50 scans with 3-ns gate time) [108]

3.4.2 Criteria for Interaction

As long as a catalyst is used below its light-off temperature, radical transfer from plasma to surface is the essence for interaction. Propagation of surface streamer can be a measure testing compatibility of the catalytic materials in plasma catalysis. A poor propagation of surface streamers indicates less interaction area that is detrimental to catalytic reactions. Figure 3.10 schematically illustrates the conditions necessary for the interactions between plasma-induced active species and catalyst surface. The dimensionless parameter Λ describes the criteria for the interaction between reactive species and the catalyst [61].

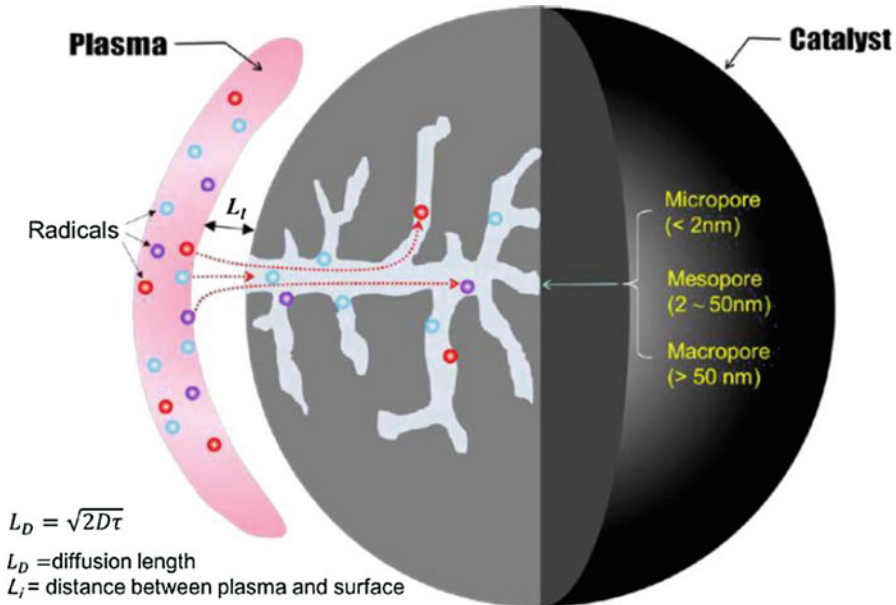


Fig. 3.10 Criteria for interaction between plasma and catalyst based on diffusion length (L_D) and distance between plasma and surface (L_1)

$$\Lambda = \frac{L_1}{L_D} \leq 1 \quad (3.3)$$

The L_D and L_1 indicate the diffusion length of reactive species and distance between the plasma and catalyst. The diffusion lengths of radicals under atmospheric pressure are about $60 \mu\text{m}$ [61]. These simple criteria indicate that the L_1 should be shorter than $60 \mu\text{m}$ to guarantee the interactions. The parameter Λ can also be applied to other plasma processes such as sterilization, plasma medicine, and surface treatment. In this regard, the closer the distance L_1 , the higher the chance for interaction between plasma and target materials (i.e., catalyst in the case of plasma catalysis).

It is clear that the presence of surface streamers and its characteristics are important factors determining good catalytic activity in plasma catalysis. Streamer imaging can be used as rough but fast tool for catalyst screening whether it is active in plasma catalysis.

3.5 Conclusion Remarks

In summary, this chapter addressed some multidisciplinary characteristics regarding interactions of NTP and catalysts possess. The effect of plasma on catalysis was discussed based on the six major particles as well as the heat. The electrical characteristics of catalysts can greatly change the properties of plasma generation. It is

therefore necessary to look at the process from multidisciplinary viewpoints to draw out useful insights into the fundamental mechanism. Especially, the recent progress on the surface streamers is presented including ns-gated time-resolved ICCD imaging. Further studies are necessary to understand the working mechanism of surface streamers and the intrinsic interactions between surface streamer and catalysts.

Acknowledgments The authors would like to acknowledge financial support from the JSPS KAKENHI Grant Number JP26400539.

References

1. Kim, H. H., Teramoto, Y., Ogata, A., Takagi, H., & Nanba, T. (2016). Plasma catalysis for environmental treatment and energy applications. *Plasma Chemistry and Plasma Processing*, 36, 45–72.
2. Penetrante, B. M., & Schultheis, S. E. (1993). *Non-thermal plasma techniques for pollution control: Part a: Overview, fundamentals and supporting technologies*. New York: Springer.
3. Penetrante, B. M., & Schultheis, S. E. (1993). *Non-thermal plasma techniques for pollution control: Part B: Electron beam and electrical discharge processing*. New York: Springer.
4. Mizuno, A., Clements, J. S., & Davis, R. H. (1986). A method for the removal of sulfur dioxide from exhaust gas utilizing pulsed streamer corona for electron energization. *IEEE Transactions on Industry Applications*, 22, 516–522.
5. Dinelli, G., Civitano, L., & Rea, M. (1990). Industrial experiments on pulsed corona simultaneous removal of NO_x and SO₂ from flue gas. *IEEE Transactions on Industry Applications*, 26, 535–541.
6. Masuda, S., & Nakao, K. (1990). Control of NO_x by positive and negative pulsed corona discharges. *IEEE Transactions on Industry Applications*, 26, 374–383.
7. Nunez, C. M., Ramsey, G. H., Ponder, W. H., Abbott, J. H., Hamel, L. E., & Kariher, P. H. (1993). Corona destruction: An innovative control technology for VOCs and air toxics. *Journal of the Air & Waste Management Association*, 42, 242–247.
8. Clements, J. S., Mizuno, A., Finney, W. C., & Davis, R. H. (1989). Combined removal of SO₂, NO_x, and fly ash from simulated flue gas using pulsed streamer corona. *IEEE Transactions on Industry Applications*, 25, 62–69.
9. Penetrante, B. M., Bardsley, J. N., & Hsiao, M. C. (1997). Kinetic analysis of non-thermal plasmas used for pollution control. *Japanese Journal of Applied Physics*, 36, 5007–5017.
10. Yamamoto, T. (1999). Optimization of nonthermal plasma for the treatment of gas streams. *Journal of Hazardous Materials*, B67, 165–181.
11. Anderegg, F. O. (1923). Surface complications in the corona discharge. *Trans. Am. Electrochemical Soc.*, 44, 203–214.
12. Yehia, A., & Mizuno, A. (2008). Suppression of the ozone generation in the positive and negative dc corona discharges. *International Journal of Plasma Environmental Science and Technology*, 2, 44–49.
13. Newsome, P. T. (1926). A study of the influence of the electrodes on the formation of ozone at low pressures in the electrical discharge. *Journal of the American Chemical Society*, 48, 2035–2045.
14. Petrov, A. A., Amirov, R. H., & Samoylov, I. S. (2009). On the nature of copper cathode erosion in negative corona discharge. *IEEE Transactions on Plasma Science*, 37, 1146–1149.
15. Dhandapani, B., & Oyama, S. T. (1997). Gas phase ozone decomposition catalysts. *Applied Catalysis B: Environmental*, 11, 129–166.
16. Henis, J. M. (1976). *Nitrogen oxide decomposition process*. USA: Monsanto Company.

17. Park, M. K., Ryu, S. G., Park, H. B., Lee, H. W., Hwang, K. C., & Lee, C. H. (2004). Decomposition of cyanogen chloride by using a packed bed plasma reactor at dry and wet air in atmospheric pressure. *Plasma Chemistry and Plasma Processing*, *24*, 117–135.
18. Chang, C. L., & Lin, T. S. (2005). Elimination of carbon monoxide in the gas streams by dielectric barrier discharge systems with Mn catalyst. *Plasma Chemistry and Plasma Processing*, *25*, 387–401.
19. Holzer, F., Kopinke, F. D., & Roland, U. (2005). Influence of ferroelectric materials and catalysts on the performance of non-thermal plasma (NTP) for the removal of air pollutants. *Plasma Chemistry and Plasma Processing*, *25*, 595–611.
20. Magureanu, M., Mandache, N. B., Parvulescu, V. I., Subrahmanyam, C., Renken, A., & Kiwi-Minsker, L. (2007). Improved performance of non-thermal plasma reactor during decomposition of trichloroethylene: Optimization of the reactor geometry and introduction of catalytic electrode. *Applied catalysis. B, Environmental*, *74*, 270–277.
21. Nozaki, T., Muto, N., Kado, S., & Okazaki, K. (2004). Dissociation of vibrationally excited methane on Ni catalyst part 1. Application to methane steam reforming. *Catalysis Today*, *89*, 57–65.
22. Kraus, M., Eliasson, B., Kogelschatz, U., & Wokaun, A. (2001). CO₂ reforming of methane by the combination of dielectric-barrier discharges and catalysis. *Physical Chemistry Chemical Physics*, *3*, 294–300.
23. Wang, Q., Yan, B. H., Jin, Y., & Cheng, Y. (2009). Dry reforming of methane in a dielectric barrier discharge reactor with Ni/Al₂O₃ catalyst: Interaction of catalyst and plasma. *Energy & Fuel*, *23*, 4196–4201.
24. Jwa, E., Lee, S. B., Lee, H. W., & Mok, Y. S. (2013). Plasma-assisted catalytic methanation of CO and CO₂ over Ni-zeolite catalysts. *Fuel Processing Technology*, *108*, 89–93.
25. Scapinello, M., Martini, L. M., & Tosi, P. (2014). CO₂ hydrogenation by CH₄ in a dielectric barrier discharge: Catalytic effects of nickel and Copper. *Plasma Processes and Polymers*, *11*, 624–628.
26. Hammer, T., & Broer, S. (1998). Plasma enhanced selective catalytic reduction of NO_x for diesel cars. Society of Automotive Engineers: Paper No. 982428.
27. Hoard, J., & Balmer, M. L. (1998). Analysis of plasma-catalysis for diesel NO_x remediation. *Society of Automotive Engineers*, *982429*, 13–19.
28. Penetrante, B. M., Brusasco, R. M., Merritt, B. T., & Vogtlin, G. E. (1999). Environmental application of low-temperature plasmas. *Pure and Applied Chemistry*, *71*, 1829–1835.
29. Kim, H. H., Takashima, K., Katsura, S., & Mizuno, A. (2001). Low-temperature NO_x reduction processes using combined systems of pulsed corona discharge and catalysts. *Journal of Physics D: Applied Physics*, *34*, 604–613.
30. Miessner, H., Francke, K.-P., Rudolph, R., & Hammer, T. (2002). NO_x removal in excess oxygen by plasma-enhanced selective catalytic reduction. *Catalysis Today*, *75*, 325–330.
31. Mok, Y. S., Dors, M., & Mizeraczyk, J. (2004). Effect of reaction temperature on NO_x removal and formation of ammonium nitrate in nonthermal plasma process combined with selective catalytic reduction. *IEEE Transactions on Plasma Science*, *32*, 799–807.
32. Patil, B., Cherkasov, N., Lang, J., Ibhaddon, A., Hessel, V., & Wang, Q. (2016). Low temperature plasma catalytic NO_x synthesis in a packed DBD reactor: Effect of support materials and supported active metal oxides. *Applied Catalysis B: Environmental*, *194*, 123–133.
33. Mizushima, T., Matsumoto, K., Sugoh, J.-I., Ohkita, H., & Kakuta, N. (2004). Tubular membrane-like catalyst for reactor with dielectric-barrier discharge plasma and its performance in ammonia synthesis. *Applied Catalysis A: General*, *265*, 53–59.
34. Hong, J., Aramesh, M., Shimoni, O., Seo, D. H., Yick, S., Greig, A., Charles, C., Prawer, S., & Murphy, A. B. (2016). Plasma catalytic synthesis of ammonia using functionalized-carbon coatings in an atmospheric-pressure non-equilibrium discharge. *Plasma Chemistry and Plasma Processing*, *36*, 917–940.
35. Kim, H. H., Teramoto, Y., Ogata, A., Takagi, H., & Nanba, T. (2017). Atmospheric-pressure nonthermal plasma synthesis of ammonia over ruthenium catalysts. *Plasma Processes and Polymers*, *14*, 1600157.

36. Vandenbroucke, A. M., Morent, R., Geyter, N. D., & Leys, C. (2011). Non-thermal plasmas for non-catalytic and catalytic VOC abatement. *Journal of Hazardous Materials*, *195*, 30–54.
37. Kusic, H., Koprivanac, N., & Locke, B. R. (2005). Decomposition of phenol by hybrid gas/liquid electrical discharge reactors with zeolite catalysts. *Journal of Hazardous Materials*, *B125*, 190–200.
38. Kim, H. H., Tsunoda, K., Katsura, S., & Mizuno, A. (1999). A novel plasma reactor for NO_x control using photocatalyst and hydrogen peroxide injection. *IEEE Transactions on Industry Applications*, *35*, 1306–1310.
39. Yoshida, H., Marui, Z., Aoyama, M., Sugiura, J., & Mizuno, A. (1989). Removal of odor gas component utilizing plasma chemical reactions promoted by the partial discharge in a ferroelectric pellet layer. *Journal of the Institute of Electrostatics Japan*, *13*, 425–430.
40. Harling, A. M., Glover, D. J., Whitehead, J. C., & Zhang, K. (2008). Novel method for enhancing the destruction of environmental pollutants by the combination of multiple plasmadischarges. *Environmental Science & Technology*, *42*, 4546–4550.
41. Park, S. Y., Deshwal, B. R., & Moon, S. H. (2008). NO_x removal from the flue gas of oil-fired boiler using a multistage plasma-catalyst hybrid system. *Fuel Processing Technology*, *89*, 540–548.
42. Hübner, M., Guaitella, O., Rousseau, A., & Röpcke, J. (2013). A spectroscopic study of ethylene destruction and by-product generation using a three-stage atmospheric packed-bed plasma reactor. *Journal of Applied Physics*, *114*, 033301.
43. Kim, H. H., Oh, S. M., Ogata, A., & Futamura, S. (2005). Decomposition of gas-phase benzene using plasma-driven catalyst reactor: Complete oxidation of adsorbed benzene using oxygen plasma. *Journal of Advanced Oxidation Technologies*, *8*, 226–233.
44. Kim, H. H., Ogata, A., & Futamura, S. (2008). Oxygen partial pressure-dependent behavior of various catalysts for the total oxidation of VOCs using cycled system of adsorption and oxygen plasma. *Applied Catalysis. B: Environmental*, *79*, 356–367.
45. Kim, H. H., Ogata, A., & Futamura, S. (2007). Complete oxidation of volatile organic compounds (VOCs) using plasma-driven catalysis and oxygen plasma. *International Journal of Plasma Environmental Science and Technology*, *1*, 46–51.
46. Fan, H. Y., Shi, C. S., Li, X. S., Zhao, D. X., Xu, Y., & Zhu, A. M. (2009). High-efficiency plasma catalytic removal of dilute benzene from air. *Journal of Physics D: Applied Physics*, *42*, 225105.
47. Fan, H. Y., Li, X. S., Shi, C., Zhao, D. Z., Liu, J. L., Liu, Y. X., & Zhu, A. M. (2011). Plasma catalytic oxidation of stored benzene in a cycled storage-discharge (CSD) process: Catalysts, reactors and operation conditions. *Plasma Chemistry and Plasma Processing*, *31*, 799–810.
48. Mok, Y. S., & Kim, D. H. (2011). Treatment of toluene by using adsorption and nonthermal plasma oxidation process. *Current Applied Physics*, *11*, S58–S62.
49. Dang, X., Huang, J., Cao, L., & Zhou, Y. (2013). Plasma-catalytic oxidation of adsorbed toluene with gas circulation. *Catalysis Communications*, *40*, 116–119.
50. Wang, W., Wang, H., Zhu, T., & Fan, X. (2015). Removal of gas phase low-concentration toluene over Mn, Ag and Cmodified HZSM-5 catalysts by periodical operation of adsorption and non-thermal plasma regeneration. *Journal of Hazardous Materials*, *292*, 70–78.
51. Qin, C., Dang, X., Huang, J., Teng, J., & Huang, X. (2016). Plasma-catalytic oxidation of adsorbed toluene on Ag-Mn/γ-Al₂O₃: Comparison of gas flow-through and gas circulation treatment. *Chemical Engineering Journal*, *299*, 85–92.
52. Zhao, D. Z., Li, X. S., Shi, C., Fan, H. Y., & Zhu, A. M. (2011). Low-concentration formaldehyde removal from air using a cycled storage-discharge (CSD) plasma catalytic process. *Chemical Engineering Science*, *66*, 3922–3929.
53. Oh, S. M., Kim, H. H., Einaga, H., Ogata, A., Futamura, S., & Park, D. W. (2006). Zeolite-combined plasma reactor for decomposition of toluene. *Thin Solid Films*, *506-507*, 418–422.
54. Kuroki, T., Hirai, K., Matsuoka, S., Kim, J. Y., & Okubo, M. (2011). Oxidation system of adsorbed VOCs on adsorbent using non thermal plasma flow. *IEEE Transactions on Industry Applications*, *47*, 1916–1921.

55. Saulich, K., & Muller, S. (2013). Removal of formaldehyde by adsorption and plasma treatment of mineral adsorbent. *Journal of Physics D: Applied Physics*, *46*, 045201.
56. Subrenat, A., Baléo, J. N., Cloirec, P. L., & Blanc, P. E. (2001). Electrical behaviour of activated carbon cloth heated by the joule effect: Desorption application. *Carbon*, *39*, 707–716.
57. Okubo, M., Inoue, M., Kuroki, T., & Yamamoto, T. (2005). NO_x reduction aftertreatment system using nitrogen nonthermal plasma desorption. *IEEE Transactions on Industry Applications*, *41*, 891–899.
58. Yoshida, K., Kuwahara, T., Kuroki, T., & Okubo, M. (2012). Diesel NO_x aftertreatment by combined process using temperature swing adsorption, NO_x reduction by nonthermal plasma, and NO_x recirculation: Improvement of the recirculation process. *Journal of Hazardous Materials*, *231-232*, 18–25.
59. Yu, Q. Q., Wang, H., Liu, T., Xiao, L. P., Jiang, X. Y., & Zheng, X. M. (2012). High-efficiency removal of NO_x using a combined adsorption-discharge plasma catalytic process. *Environmental Science & Technology*, *46*, 2337–2344.
60. Kim, H. H., Prieto, G., Takashima, K., Katsura, S., & Mizuno, A. (2002). Performance evaluation of discharge plasma process for gaseous pollutant removal. *Journal of Electrostatics*, *55*, 25–41.
61. Kim, H. H., Teramoto, Y., Negishi, N., & Ogata, A. (2015). A multidisciplinary approach to understand the interactions of nonthermal plasma and catalyst: A review. *Catalysis Today*, *256*, 13–22.
62. Francke, K. P., Rudolph, R., & Miessner, H. (2003). Design and operation characteristics of a simple and reliable DBD reactor for use with atmospheric air. *Plasma Chemistry and Plasma Processing*, *23*, 47–57.
63. Kogelschatz, U. (2003). Dielectric-barrier discharges: Their history, discharge physics, and industrial applications. *Plasma Chemistry and Plasma Processing*, *23*, 1–46.
64. Kim, H. H., & Ogata, A. (2012). Interaction of nonthermal plasma with catalyst for the air pollution control. *International Journal of Plasma Environmental Science and Technology*, *6*, 43–48.
65. Mizuno, A., & Ito, H. (1990). Basic performance of an electrostatically augmented filter consisting of a packed ferroelectric pellet layer. *Journal of Electrostatics*, *25*, 97–107.
66. Harling, A. M., Kim, H. H., Futamura, S., & Whitehead, J. C. (2007). Temperature dependence of plasma-catalysis using a nonthermal, atmospheric pressure packed bed; the destruction of benzene and toluene. *Journal of Physical Chemistry C*, *111*, 5090–5095.
67. Kim, H. H., Teramoto, Y., Sano, T., Negishi, N., & Ogata, A. (2015). Effects of Si/Al ratio on the interaction of nonthermal plasma and Ag/HY catalysts. *Applied Catalysis B: Environmental*, *166-167*, 9–17.
68. Kuai, P.-Y., Liu, C.-J., & Huo, P.-P. (2009). Characterization of CuO-ZnO catalyst prepared by decomposition of carbonates using dielectric-barrier discharge plasma. *Catalysis Letters*, *129*, 493–498.
69. Liu, Y., Pan, Y.-X., Kuai, P., & Liu, C.-J. (2010). Template removal from ZSM-5 zeolite using dielectric-barrier discharge plasma. *Catalysis Letters*, *135*, 241–251.
70. Tu, X., Gallon, H. J., & Whitehead, J. C. (2013). Plasma-assisted reduction of a NiO/Al₂O₃ catalyst in atmospheric pressure H₂/Ar dielectric barrier discharge. *Catalysis Today*, *211*, 120–125.
71. Kim, T., Lee, D. H., Jo, S. K., Pyun, S. H., Kim, K. T., & Song, Y. H. (2016). Mechanism of the accelerated reduction of an oxidized metal catalyst under electric discharge. *ChemCatChem*, *8*, 685–689.
72. Liu, X., Mou, C. Y., Lee, S., Li, Y., Secrest, J., & Jang, B. W. L. (2012). Room temperature O₂ plasma treatment of SiO₂ supported Au catalysts for selective hydrogenation of acetylene in the presence of large excess of ethylene. *Journal of Catalysis*, *285*, 152–159.
73. Liu, C. J., Zhao, Y., Li, Y., Zhang, D. S., Chang, Z., & Bu, W. H. (2013). Perspectives on electron-assisted reduction for preparation of highly dispersed noble metal catalysts. *ACS Sustainable Chemistry & Engineering*, *2*, 3–13.

74. Menard, L. D., Xu, F., Nuzzo, R. G., & Yang, J. C. (2006). Preparation of TiO₂-supported Au nanoparticle catalysts from a Au₁₃ cluster precursor: Ligand removal using ozone exposure versus a rapid thermal treatment. *Journal of Catalysis*, *243*, 64–73.
75. Khan, M. A., & Al-Jalal, A. A. (2004). Enhanced decoking of a coked zeolite catalyst using a glow discharge in Ar-O₂ gas mixture. *Applied Catalysis A: General*, *272*, 141–149.
76. Al-Jalal, A. M., & Khan, M. A. (2010). Optical emission and raman spectroscopy studies of reactivity of low-pressure glow discharges in Ar-O₂ and He-O₂ gas mixtures with coked catalysts. *Plasma Chemistry and Plasma Processing*, *30*, 173–182.
77. Kim, H. H., Tsubota, S., Daté, M., Ogata, A., & Futamura, S. (2007). Catalyst regeneration and activity enhancement of Au/TiO₂ by atmospheric pressure nonthermal plasma. *Applied Catalysis A: General*, *329*, 93–98.
78. Fan, H. Y., Shi, C. A., Li, X. S., Zhang, S., Liu, J. L., & Zhu, A. M. (2012). In-situ plasma regeneration of deactivated Au/TiO₂ nanocatalysts during CO oxidation and effect of N₂ content. *Applied Catalysis B: Environmental*, *119*, 49–55.
79. Yoshida, H., Kuwauchi, Y., Jinschek, J. R., Sun, K., Tanaka, S., Kohyama, M., Shimada, S., Haruta, M., & Takeda, S. (2012). Visualizing gas molecules interacting with supported nanoparticulate catalysts at reaction conditions. *Science*, *335*, 317–320.
80. Somorjai, G. A. (1992). The experimental evidence of the role of surface restructuring during catalytic reactions. *Catalysis Letters*, *12*, 17–34.
81. Sano, T., Negishi, N., Sakai, E., & Matsuzawa, S. (2006). Contributions of photocatalytic/catalytic activities of TiO₂ and γ -Al₂O₃ in nonthermal plasma on oxidation of acetaldehyde and CO. *Journal of Molecular Catalysis A: Chemical*, *245*, 235–241.
82. Rajasekaran, P., Mertmann, P., Bibinov, N., Wandke, D., Viol, W., & Awakovicz, P. (2010). Filamentary and homogeneous modes of dielectric barrier discharge (DBD) in air: Investigation through plasma characterization and simulation of surface irradiation. *Plasma Processes and Polymers*, *7*, 665–675.
83. Ochiai, T., Nakata, K., Murakami, T., Morito, Y., Hosokawa, S., & Fusishima, A. (2011). Development of an air-purification unit using a photocatalysis-plasma hybrid reactor. *Electrochemistry*, *79*, 838–841.
84. Huang, H. B., Ye, D. Q., Fu, M. L., & Feng, F. D. (2007). Contribution of UV light to the decomposition of toluene in dielectric barrier discharge plasma/photocatalysis system. *Plasma Chemistry and Plasma Processing*, *27*, 577–588.
85. Maciucă, A., Batiot-Dupeyrat, C., & Tatibouet, J. M. (2012). Synergetic effect by coupling photocatalysis with plasma for low VOCs concentration removal from air. *Applied Catalysis B: Environmental*, *125*, 432–438.
86. Ono, R. (2016). Optical diagnostics of reactive species in atmospheric-pressure nonthermal plasma. *Journal of Physics D: Applied Physics*, *49*, 083001.
87. Guaitella, O., Lazzaroni, C., Marinov, D., & Rousseau, A. (2010). Evidence of atomic adsorption on TiO₂ under plasma exposure and related C₂H₂ surface reactivity. *Applied Physics Letters*, *97*, 011502.
88. Marinov, D., Guaitella, O., Rousseau, A., & Ionikh, Y. (2010). Production of molecules on a surface under plasma exposure: Example of NO on pyrex. *Journal of Physics D: Applied Physics*, *43*, 115203.
89. Kim, H. H., Ogata, A., Schiorlin, M., Marotta, E., & Paradisi, C. (2011). Oxygen isotope (¹⁸O₂) evidence on the role of oxygen in the plasma-driven catalysis of VOC oxidation. *Catalysis Letters*, *141*, 277–282.
90. Teramoto, Y., Kim, H. H., Ogata, A., & Negishi, N. (2013). Study of plasma-induced surface active oxygen on zeolite-supported silver nanoparticles. *Catalysis Letters*, *143*, 1374–1378.
91. Guaitella, O., Hubner, M., Welzel, S., Marinov, D., Ropcke, J., & Rousseau, A. (2010). Evidence for surface oxidation on pyrex of NO into NO₂ by adsorbed O atoms. *Plasma Sources Science and Technology*, *19*, 045206.
92. Biener, J., Wittstock, A., Zepeda-Ruiz, L. A., Biener, M. M., Zielasek, V., Kramer, D., Viswanath, R. N., Weissmüller, J., Bäumer, M., & Hamza, A. V. (2009). Surface-chemistry-driven actuation in nanoporous gold. *Nature Materials*, *8*, 47–51.

93. Utz, A. L. (2009). Mode selective chemistry at surfaces. *Current Opinion in Solid State & Materials Science*, 13, 4–12.
94. Nozaki, T., Muto, N., Kadio, S., & Okazaki, K. (2004). Dissociation of vibrationally excited methane on Ni catalyst part 2. Process diagnostics by emission spectroscopy. *Catalysis Today*, 89, 67–74.
95. Haruta, M., Yamada, N., Kobayashi, T., & Iijima, S. (1989). Gold catalysts prepared by coprecipitation for low-temperature oxidation of hydrogen and of carbon monoxide. *Journal of Catalysis*, 115, 301–309.
96. Jiang, C., Hara, K., & Fukuoka, A. (2013). Low-temperature oxidation of ethylene over platinum nanoparticles supported on mesoporous silica. *Angewandte Chemie, International Edition*, 52, 6265–6268.
97. Stere, C. E., Adress, W., Burch, R., Chansai, S., Goguet, A., Graham, W. G., & Hardacre, C. (2015). Probing a non-thermal plasma activated heterogeneously catalyzed reaction using in situ DRIFTS-MS. *ACS Catalysis*, 5, 956–964.
98. Rodrigues, A., Tatibouet, J. M., & Fourre, E. (2016). Operando DRIFT spectroscopy characterization of intermediate species on catalysts surface in VOC removal from air by non-thermal plasma assisted catalysis. *Plasma Chemistry and Plasma Processing*, 36, 901–915.
99. Su, H., & Yeung, E. S. (2000). High-throughput screening of heterogeneous catalysts by laser-induced fluorescence imaging. *Journal of the American Chemical Society*, 122, 7422–7423.
100. Su, H., Hou, Y., Houk, R. S., Schrader, G. L., & Yeung, E. S. (2001). Combinatorial screening of heterogeneous catalysts in selective oxidation of naphthalene by laser-induced fluorescence imaging. *Analytical Chemistry*, 73, 4434–4440.
101. Kim, H. H., Kim, J. H., & Ogata, A. (2009). Microscopic observation of discharge plasma on the surface of zeolites supported metal nanoparticles. *Journal of Physics D: Applied Physics*, 42, 135210.
102. Kim, H. H., & Ogata, A. (2011). Nonthermal plasma activates catalyst: From current understanding and future prospects. *European Physical Journal Applied Physics*, 55, 13806.
103. Mizuno, A., Yamazaki, Y., Ito, H., & Yoshida, H. (1992). Ac energized ferroelectric pellet bed gas cleaner. *IEEE Transactions on Industry Applications*, 28, 535–540.
104. Mizuno, A., Yamazaki, Y., Obama, S., Suzuki, E., & Okazaki, K. (1993). Effect of voltage waveform on partial discharge in ferroelectric pellet layer for gas cleaning. *IEEE Transactions on Industry Applications*, 29, 262–267.
105. Takaki, K., Chang, J. S., & Kostov, K. G. (2004). Atmospheric pressure of nitrogen plasmas in a ferro-electric packed bed barrier discharge reactor part I: Modeling. *IEEE Transactions on Dielectrics and Electrical Insulation*, 11, 481–490.
106. Nozaki, T., Unno, Y., Miyazaki, Y., & Okazaki, K. (2001). Optical diagnostics for determining gas temperature of reactive microdischarges in a methane-fed dielectric barrier discharge. *Journal of Physics D: Applied Physics*, 34, 2504–2511.
107. Hofst, H., Kettlitz, M., Weltmann, K.-D., & Brandenburg, R. (2014). The bidirectional character of O₂ concentration in pulsed dielectric barrier discharges in O₂/N₂ gas mixtures. *Journal of Physics D: Applied Physics*, 47, 455202.
108. Kim, H. H., Teramoto, Y., & Ogata, A. (2016). Time-resolved imaging of positive pulsed corona-induced surface streamers on TiO₂ and γ -Al₂O₃-supported Ag catalysts. *Journal of Physics D: Applied Physics*, 49, 415204.
109. Marode, E. (1975). The mechanism of spark breakdown in air at atmospheric pressure between a positive point and a plane. 1. Experimental: Nature of the streamer track. *Journal of Applied Physics*, 46, 2005–2015.
110. Namihira, T., Wang, D., Katsuki, S., Hackam, R., & Akiyama, H. (2003). Propagation velocity of pulsed streamer discharges in atmospheric air. *IEEE Transactions on Plasma Science*, 31, 1091–1094.
111. Huiskamp, T., Pemen, A. J. M., Hoeben, W. F. L. M., Beckers, F. J. C. M., & Heesch, E. J. M. V. (2013). Temperature and pressure effects on positive streamers in air. *Journal of Physics D: Applied Physics*, 46, 165202.